Tribol Lett (2014) 53:411–420
DOI 10.1007/s11249-013-0280-1

ORIGINAL PAPER

Watershed-Based Morphological Separation of Wear Debris Chains for On-Line Ferrograph Analysis

Hongkun Wu · Tonghai Wu · Yeping Peng · Zhongxiao Peng

Received: 15 October 2013 / Accepted: 6 December 2013 / Published online: 13 December 2013

Abstract Separation and characterization of wear debris from ferrograph images are demanded for on-line analysis. However, particle overlapping issue associated with wear debris chains has markedly limited this technique due to the difficulty in effectively segmenting individual particles from the chains. To solve this bottleneck problem, studies were conducted in this paper to establish a practical method for wear debris separation for on-line analysis. Two conventional watershed approaches were attempted. Accordingly, distance-based transformation had a problem with oversegmentation, which led to overcounting of wear debris. Another method, by integrating the ultimate corrosion and condition expansion (UCCE), introduced boundary-offset errors that unavoidably affected the boundary identification between particles, while varying the corrosion scales and adopting a low-pass filtering method improved the UCCE with satisfactory results. Finally, together with a termination criterion, an automatic identification process was applied with real on-line wear debris images sampled from a mineral scraper gearbox. With the satisfactory separation result, several parameters for characterization were extracted and some statistics were constructed to obtain an overall evaluation of existing particles. The proposed method shows a promising prospect in on-line wear monitoring with deep insight into wear mechanism.

H. Wu · T. Wu (✉) · Y. Peng
Key Laboratory of Education Ministry for Modern Design and Rotor-Bearing System, Xi'an Jiaotong University, Xi'an 710049, China
e-mail: wt-h@163.com

T. Wu · Z. Peng
School of Mechanical and Manufacturing Engineering, The University of New South Wales, Sydney, Australia

Keywords Wear debris analysis · Ferrograph image · On-line monitoring · Wear characterization

1 Introduction

Recently, there is an increasing demand for real-time condition monitoring to cope with the growing complexities of modern machinery. Condition-based maintenance (CBM) using on-line monitoring techniques has been a popular practice in reducing maintenance costs and maintaining long-term reliability [1]. Wear debris, as by-products of wear processes, has been correlated with the cause of machine deterioration and thus used as information sources for wear characterization. Wear debris analysis carried out by analytical and filter ferrography [2] with imaging technology [3] has served as one of the most commonly used techniques for machine condition monitoring and faults diagnosis [4]. Particularly, images of wear debris are valuable resources for evaluating wear rates and for examining wear mechanisms [3]. Many researchers have used high-resolution instruments to investigate the fine features of individual wear debris in two dimension (2D) and three dimension (3D), and to study the wear mechanisms and evolving degradation of machine parts [4–7]. However, identifying and separating representative wear debris from an image can be difficult and are usually accomplished by operator's intuition and experience. Indeed, it is a time-consuming task to identify individual particles from a cluster of wear debris, especially when ferrography is used to collect the debris, so a traditional analysis of wear debris is constrained from progressing toward a rapid and automatic method [8].

On-line analysis of wear debris to monitor a machine's performance over its full lifetime has become promising, particularly with the advancement of sensor techniques for on-line image acquisition techniques [9]. Unfortunately, the existing on-line systems use a method similar to analytical ferrography to collect and analyze wear debris, and this approach introduces a problem with particle overlap and makes it difficult to identify individual particles [3]. Generally, wear debris in a ferrograph image reveals complex patterns, such as chains and clusters, due to the microattraction forces among these ferroparticles under the necessarily applied magnetic field [10]. Although computer-aided analysis has been applied to individual wear debris, separating the debris from their existing patterns remains a challenge [11], so some morphological methods were investigated to improve the effect of automatic segmentation [12]. Of these methods, watershed method has been studied extensively because it is very reliable and extremely efficient in different situations [13]. A popular watershed method, distance-based transformation, uses the principle of flooded terrain to obtain watershed ridge lines for segmentation by applying a distance transformation on a binary image [14]. However, such method is sensitive to the details of images and is subject to oversegmentation. Concave point assignment is another morphological method used to separate two round particles sticking together. Here, two concave points pointing toward the outside of a closed shape are adopted, and a rational division can be achieved by finding the correct line connecting the two concave points. However, this algorithm has been reported with a low accuracy of below 85 % [15]. Moreover, it strictly requires objects of regular shape, which is not available in most cases in wear debris analysis. Another method, separated search point, has provided good performance in closed area separation. In this method, small areas were separated in an image after continuously implementing corrosion process. The breaking points of separation constitute to the final dividing line of the separated area [16]. Acceptable results by this method have been obtained from segmenting cells and grains due to their intrinsic morphological advantages such as circle similarity, closed size distribution, and smooth margins.

Wear debris images separation, due to their highly irregularity shapes and aggregations, has become the bottleneck in on-line ferrograph applications. In this paper, wear debris chains segmentation with on-line images was investigated for automatic ferrograph analysis. A morphological separation was carried out by applying two watershed transformations, distance based and corrosion expansion. Their limitations are presented, and special efforts were paid on the improvement of corrosion-expansion method. Finally, a self-adaptive method has been proposed guaranteeing acceptable separation outcomes for on-line wear debris images.

2 A Mathematical and Morphological Separation of the Wear Debris Chain

Separating the wear debris can generally be attributed to segmentation of overlapping particles. Generally, both gray and morphology information can be utilized in the separation of particles. Gray-based methods with the watershed segmentation algorithm [17–19] have been reported in the separation of grain particles in gray images with high resolution. Attempts were made to identify different types of metal debris from an on-line ferrograph image by their contrasting colors. However, as Fig. 1 shows, on-line images are often noisy and have a low resolution (which is 640×480), so it is more feasible to extract their morphological characteristics than gray ones. Indeed, with such a low resolution, only images with larger wear debris can be analyzed, for example in severe wear cases. Correspondingly, typical on-line transmitted ferrograph images in Fig. 1 were taken from on-line monitoring samples of a mine scraper conveyor gearbox that was made from carbon steel.

In addition, two distinctive features of on-line chains of wear debris should be noted, the highly irregular shapes of debris and the large diversity in their sizes. On the other hand, watershed transformation having been proven with high robustness for detailed separation would be an attractive solution method. Furthermore, there are various watershed transformations based on different mathematical principles that can be considered as a suitable approach for the wear debris separation problem.

2.1 Distance-Transform-Based Watershed Segmentation

Watershed segmentation using distance transform was first used for wear debris chain segmentation in this study. A typical image with a chain of multiple wear particles, taken from Fig. 1a and shown in Fig. 2a, was used as a demonstration. By visual inspection, four wear particles were

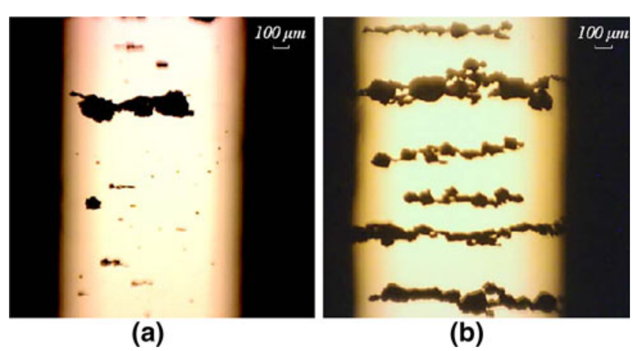

Fig. 1 Typical on-line transmitted ferrograph images with different patterns: **a** simple chains, **b** complex clusters

identified from the chain approximately. To eliminate the influence of fine features such as holes or spikes, morphological filtering [20] was performed on the image, and it was then converted into its binary form as shown in Fig. 2b.

By the principle of distance-transform-based watershed method [14], the distance and distribution of the pixels in the image were obtained by calculating the distances of each pixel from the boundary to the centroid of the wear debris chain, as shown in Fig. 3a, where the distance was represented by the gray magnitude of the pixel. Watershed ridge lines were then extracted using distance transformation; the result is shown in Fig. 3b. The final separation was achieved by superimposing the ridge lines on the original images and is illustrated in Fig. 3c.

It was observed that several redundant areas were separated due to some split ridge lines (circled in red in the Figure). By taking the No. 2 wear debris in Fig. 2a as an example, three ridge lines were generated, which resulted in at least four additional separated areas. This situation was defined as oversegmentation, by referring to the additional and unwanted areas during the separation process.

2.2 Ultimate Corrosion-Conditional Expansion Separation

The combination of extreme corrosion and conditional expansion was reported in the morphological separation of debris in off-line ferrograph image [12]. Corrosion means to eliminate the outer pixels of the wear debris by layers with a specific structural matrix element used to identify the eliminated layer of pixels. The size of the matrix element determines the number of pixels to be corroded for each cycle of corrosion, and the number of cycles needed to complete one separation is defined as the *corrosion scale*, which determines not only the remaining area but also the corrosion rate. Accordingly, by constantly eroding the area of wear debris chains in on-line images, the sticking areas are continuously reduced in size until they are eventually separated. In extreme cases, each separated area would be eroded until it vanished, should the condition for termination not be specified. Thus, the corrosion should be terminated when the objective area is small enough and approaching completely vanishing. The remaining area is then defined as the *core* of the separated area. The core marks the centers of potential wear debris, and the quantity of overall cores denotes the number of separated debris. In this example case, four separated cores of wear debris image are shown in Fig. 4a.

Eroding an area to a core with a size that is similar to the structural element has been defined as ultimate corrosion. Ultimate corrosion helps to find the centroid of the wear debris, and the conditional expansion is carried out to obtain the full shape of the wear debris by expanding the area from the core with two predefined conditions as:

1. Not exceeding the boundaries of the initial wear debris chains and
2. No overlapping or contact between the separated areas.

Thus, dividing lines between adjacent wear debris were obtained by connecting their meeting points. Figure 4b

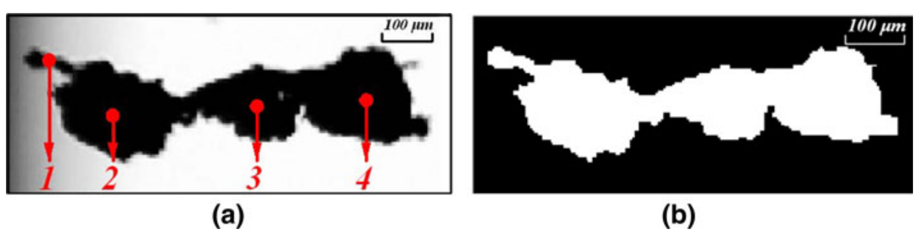

Fig. 2 Initial and processed image of a selected wear debris chain from Fig. 1a: **a** initial *gray* chain image with four intuitively identified wear debris, **b** binary chain image

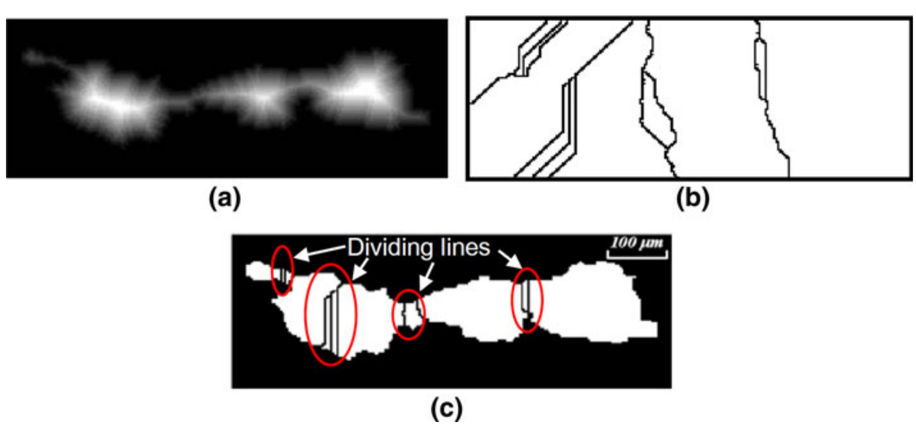

Fig. 3 Distance-based transform processes of selected wear debris chain in Fig. 2: **a** distance distribution, **b** dividing lines, **c** separation result

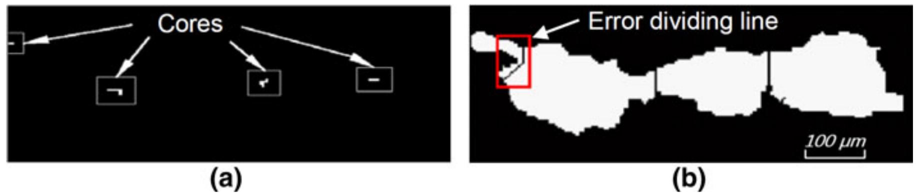

Fig. 4 Wear debris separation with ultimate corrosion-conditional expansion (UCCE): **a** cores after ultimate corrosion, **b** result of separation after conditional expansion

shows the separation result of Fig. 2a by applying the ultimate corrosion-conditional expansion (UCCE) procedure mentioned above. Referring to Fig. 2a, the dividing line in Fig. 4b between the No. 1 and No. 2 wear debris was mistakenly identified because it tended to be close to the larger particle, whereas this problem was not reported in the cell separation because the cells are usually similar in size.

The effect of the size difference on particle separation was analyzed and is illustrated in Fig. 5. For round particles such as cells, as shown in Fig. 5a, most sticking areas were in similar circles, and when they were expanded from two cores at the same rate, there were two inflated contact areas at the dividing boundary, and therefore, a rational separation was achieved. With the wear debris shown in Fig. 5b, the dimension of the particles varied widely, so when they were from the two cores at the same rate, the dividing boundary partly favored the larger one. Therefore, dividing lines tended to attach to the larger wear debris when their sizes were different.

Accordingly, the main problems of the UCCE method for wear debris separation were recognized as follows. Extreme corrosion unavoidably led to overcorrosion even if a good separation was obtained, which in turn introduced a deviation of dividing lines during expansion. Evidently, the elementary UCCE method could not maintain high separation accuracy for wear debris images.

3 Improvement of the Corrosion-Expansion Method

3.1 Uniform Scale Corrosion and Conditional Expansion (USCCE)

A controllable approach to corrosion was proposed to relax the limitations of UCCE. In the suggested modification, corrosion was carried out with a uniform scale regardless of the size of an objective area, and it was terminated when a small area was separated. Next, a conditional expansion of the separated areas was carried out to obtain dividing lines. In this way, both the separated larger and smaller areas evolved with uniform corrosion cycles (This cycle is equal to the scale mentioned below), and thus expansion cycles would become uniform. This process is called uniform scale corrosion and conditional expansion (USCCE), by which two different sized particles were correctly divided.

The USCCE method was applied to the image shown in Fig. 2. As seen from Fig. 6a, b, after two corrosions, a small amount of wear debris was gradually isolated from the rest of the aggregate. Conditional expansion was conducted for both the larger and smaller separated areas; a reasonable dividing line was obtained as shown in Fig. 6c.

The improved USCCE was able to achieve correct dividing lines between areas with different dimensions. However, it was noticed from Fig. 6 that the small area (marked by the red rectangle in Fig. 6c) was separated, while the larger area remained attached together. If USCCE was used to separate the larger areas, repeated corrosions in a larger scale would be required. As Fig. 7 shows, large scale corrosions resulted in smaller areas to vanish after a number of corrosion processes. Therefore, the main limitation of USCCE was due to incomplete separation, and this is caused by applying the same scale to separate both large and small areas of wear debris simultaneously.

3.2 Multi-Scale Corrosion and Conditional Expansion

In order to resolve the above-identified problem with USCCE, varying scales were adopted in corroding large and small debris separately. Practically, a multi-scale corrosion and conditional expansion (MSCCE) method was proposed as illustrated in Fig. 8.

As see in Fig. 8, a wear debris like chain consists of three aggregated particles in different sizes. The number of connected areas (NCA) was adopted as an indicator to count separated debris. Generally, when applying varied scales for each corrosion, several cycles of corrosion expansion were required for a satisfied separation outcome due to the wide diversity of wear debris size. At the initial cycle, a small corrosion scale was adopted for smaller debris to avoid overcorrosion. The value of NCA increased with the appearance of one core value obtained through corrosion. Conditional expansion was carried out with the identified cores and terminated by some predefined conditions. Consequently, the dividing line of the initial scale located between the separated and initial area was obtained by subtracting the initial image from the expansion result. After further cycles of separation of small wear debris, the

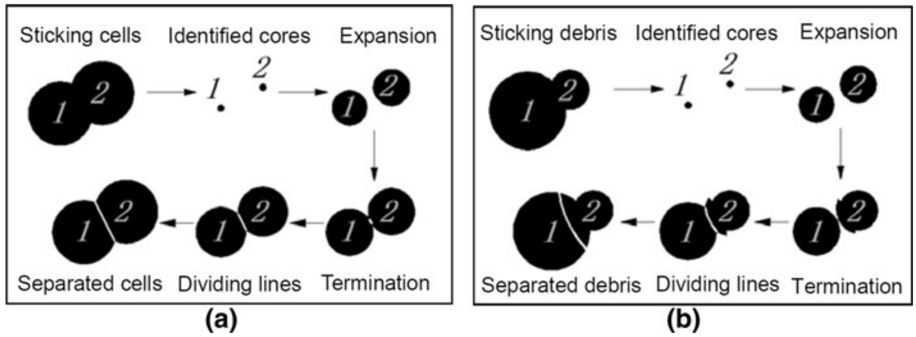

Fig. 5 Principle of generating the error dividing lines for separating the wear debris, compared to separating the cells: **a** separating the cell, **b** separating the wear debris

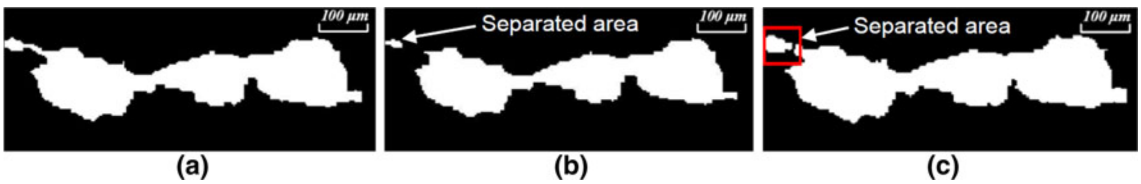

Fig. 6 Corrosion-expansion process with fixed small scale: **a** after 1st corrosion, **b** after 2nd corrosion, **c** after conditional expansion

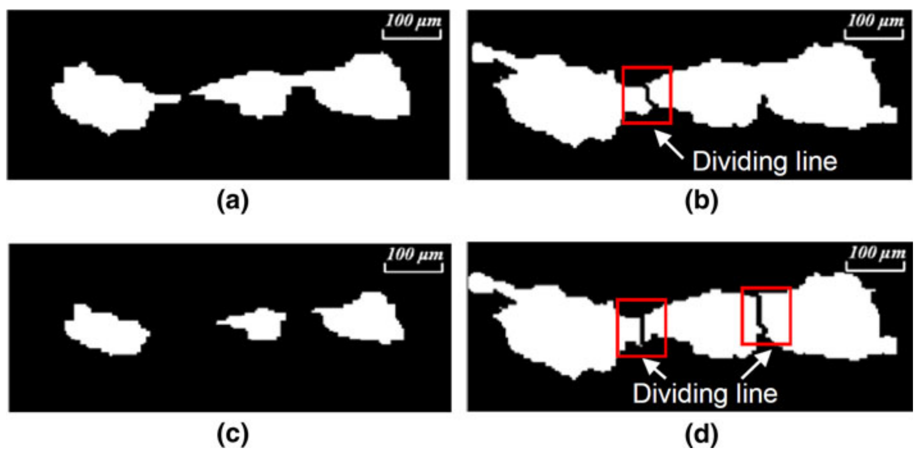

Fig. 7 Corrosion-expansion process at a fixed large scale: **a** after 4th corrosion, **b** after conditional expansion, **c** after 7th corrosion, **d** after conditional expansion

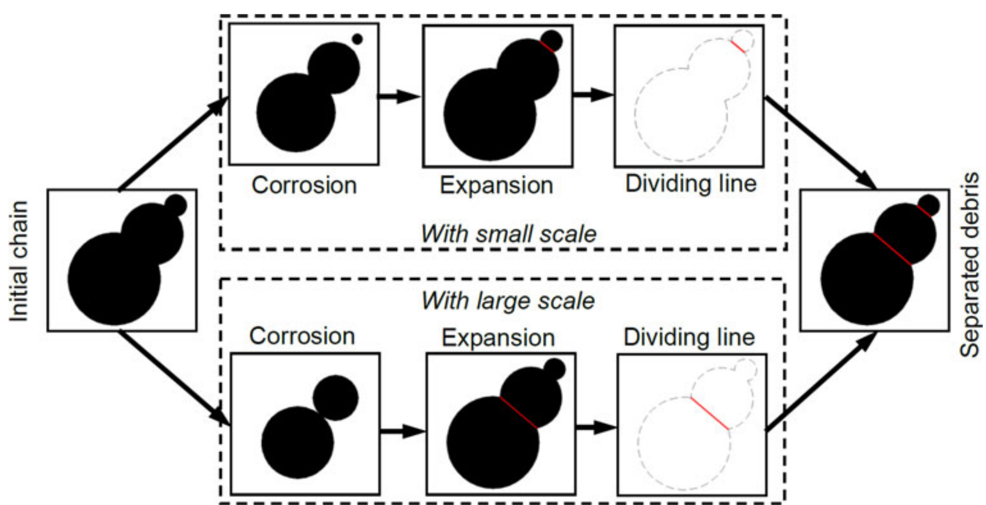

Fig. 8 Strategy of multi-scale corrosion-expansion separation of wear debris chain

larger scales for corrosion were adopted. In this stage, only larger wear debris was concerned. Finally, three particles were separated from the initial chain by gathering the dividing lines of different scales.

The termination criterion for the overall process was defined as when no additional areas appeared during successive corrosions. Therefore, the total number of areas was used as the indicator. Practically, when corroding a large area with a large scale, some smaller areas would vanish before the larger one was completely isolated. This phenomenon indicated that the number of separated areas did not always increase during corrosion, but would even decrease in many cases after the separation cycles. Therefore, a practical criterion was formulated by considering both increasing and decreasing cases, as illustrated in Fig. 9.

In each corrosion cycle, the number of disappeared areas was recorded by $\mathrm{NUM_{dis}}$, the increment in actual areas by $\mathrm{NUM_{add}}$, and the total number of separated areas in the previous cycle was denoted by $\mathrm{NUM_{total-0}}$. Consequently, the number of overall separated areas denoted by $\mathrm{NUM_{total-1}}$ can be calculated as:

$$\mathrm{NUM_{total-1}} = \mathrm{NUM_{total-0}} - \mathrm{NUM_{dis}} + \mathrm{NUM_{add}}$$

Then, the increment in actual areas $\mathrm{NUM_{add}}$ was obtained as

$$\mathrm{NUM_{add}} = \mathrm{NUM_{total-1}} - (\mathrm{NUM_{total-0}} - \mathrm{NUM_{dis}})$$

With the above definition, it was concluded that a new and separated area emerged with the indicator $\mathrm{NUM_{add}} > 0$. Thus, new dividing lines can be obtained.

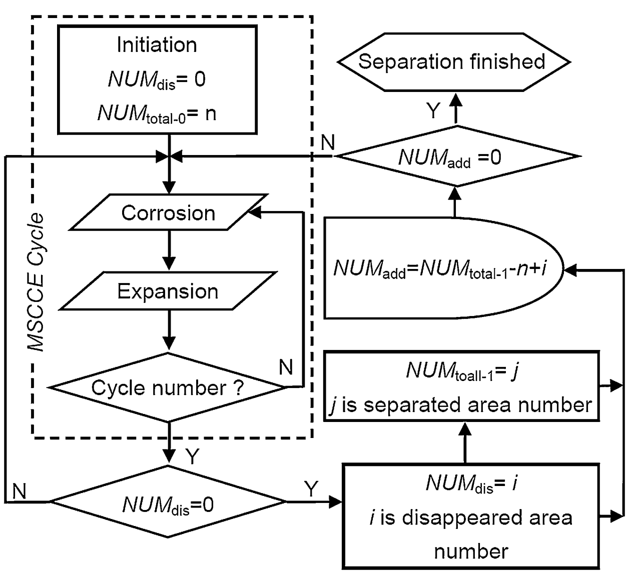

Fig. 9 Termination principle of wear debris separation process for an on-line image. NUM_{dis}, the number of areas that disappeared, NUM_{add}, the increment in actual areas, $NUM_{total-0}$, the total number of separated areas in the previous cycle, $NUM_{total-1}$, the number of overall separated areas, and *MSCCE*, multi-scale corrosion and conditional expansion

Practically, $\mathrm{NUM_{add}}$ was obtained in a two-steps process. The first step was to identify all the areas that would disappear in the current cycle with an area threshold and the number of these areas was saved as $\mathrm{NUM_{dis}}$, and the second step was to go back to the previously adjacent cycle and to eliminate those areas already identified. Hence, the actual increment in the areas was accurately obtained in the current image. By monitoring the variation in the increment in the actual areas, $\mathrm{NUM_{add}}$, the overall process for wear debris chain segmentation was terminated.

Specially, this method was applied to the automatic separation of the on-line wear debris chain in Fig. 2. After aforementioned filtering process, the image was processed using the MSCCE method. Figure 10 shows the results for each separation cycle of the overall process.

As seen in Fig. 10, wear debris of different size was processed cyclically with different scales. Evidently, the smaller wear debris was separated first, followed by larger ones. With full dividing lines, all wear particles were separated as shown in Fig. 10k. The overall process was carried out automatically. Figure 11 shows the variation in the number of identified wear debris with cycle numbers. After 7 cycles, the number of the overall identified wear debris became constant and no more area emerged under continued corrosion, and the separation was terminated.

3.3 Post-Processing

Although the separation accuracy was improved with the MSCCE method, overseparation to a certain degree is unavoidable. As seen from Fig. 10k, an extra small area, close to No. 2 and No. 3 wear debris, emerged after the final corrosion cycle, which could be judged intuitively as a false debris which was actually an additional area generated by separation. This error increased counted small particles. The source of these errors could be examined by tracing the unexpected dividing lines during the corrosion cycles. In fact, large areas were applied simultaneous corrosion in the early corrosion cycles for small areas. Although they were not separated completely, some extra small protruding areas could be isolated after cycles of corrosions. With accumulation of such occurrence, several dividing lines were generated in the same area corresponding to different corrosion scales. Eventually, extra small areas eventually appeared, as shown in Fig. 10k.

Generally, such additional area was relatively small and had no significant influence on the features of larger wear debris from which they were separated. Thus, a low-pass filter with an area threshold was adopted to remove the small areas. However, small areas could also indicate real wear debris. As mentioned above, small wear debris was always separated at the initial cycles, while extra areas were generated at later cycles. By marking and saving the

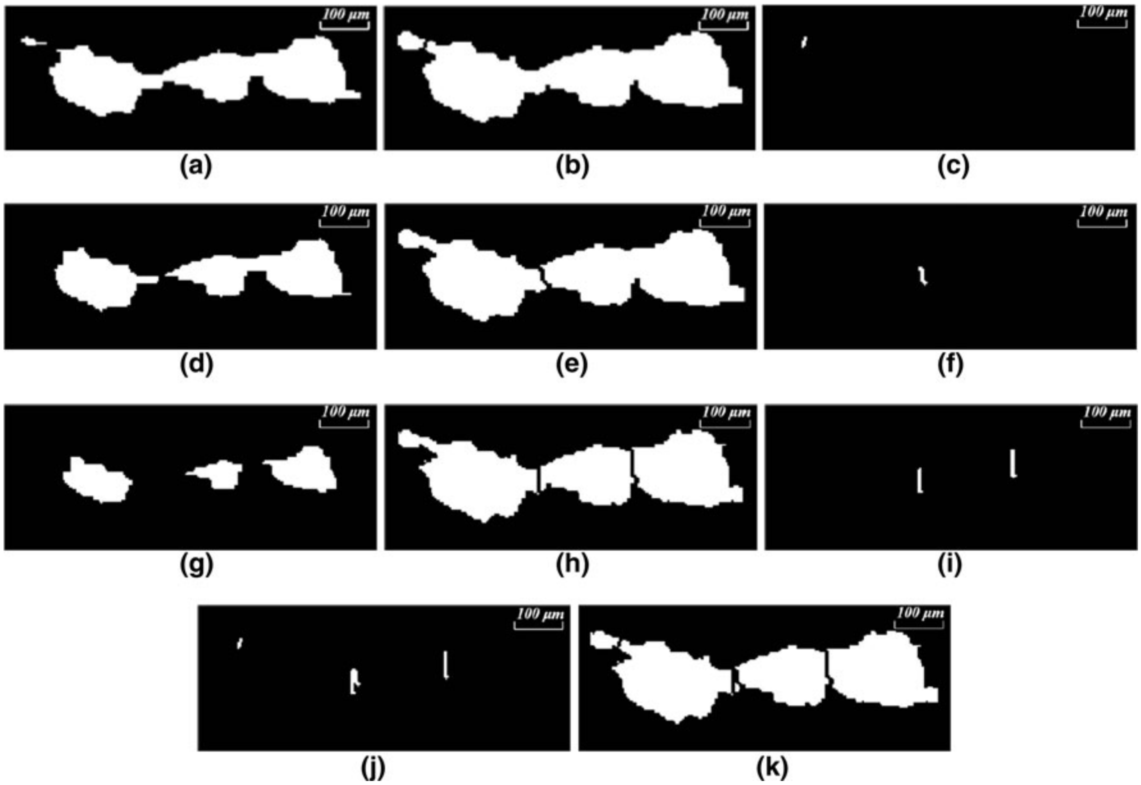

Fig. 10 Key results of an overall separation process of the wear debris chain with an improved multi-scale corrosion-expansion method: **a** the corrosion number = 2, **b** after the 1st expansion, **c** the 1st dividing line, **d** corrosion number = 4, **e** after 2nd expansion, **f** the 2nd dividing line, **g** corrosion number = 7, **h** after 3rd expansion, **i** the 3rd dividing line, **j** Overall dividing lines, and **k** final separation result

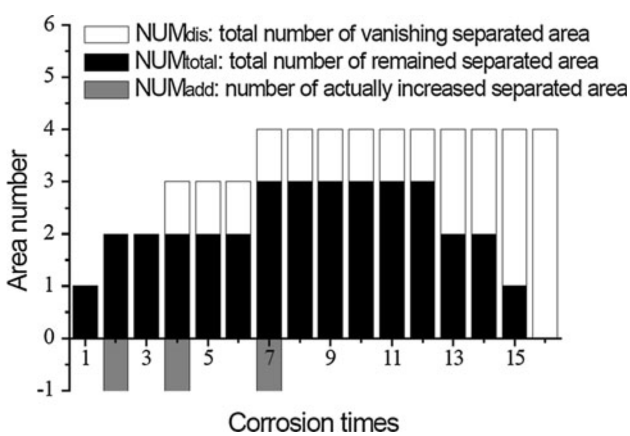

Fig. 11 Evolution of separated areas number calculated for termination

small areas in the former cycles using a filter with certain threshold, the real small debris could be preserved while the additional smaller areas were erased. The comparison between before and after the area-based filtration is shown in Fig. 12a, b.

With the suggested post-processing, the problem of a small areas emerging inaccurately was eliminated, and thus, the small debris was separated satisfactorily.

4 Application and Discussion

Both the accuracy and efficiency of the above-mentioned MSCCE method were taken into consideration in this work. High efficiency was maintained by applying the automatic particle separation approach for on-line monitoring. Meanwhile, high accuracy was achieved by using the combination of MSCCE and post-processing filtration. Furthermore, the accuracy of the proposed algorithms was essentially determined by the termination criterion where the current best result is produced, see Fig. 11. However, in the case of a complicated pattern of wear debris chains as shown in Fig. 1b, applying the above termination criterion increased the overall convergence time of the algorithm when there was a large amount of small wear debris in an image. A solution for this problem was proposed by combining unexpected small areas with a predefined threshold. However, an early convergence would occur if some larger wear debris exists, making it difficult to achieve full separation of the overall wear debris.

An alternative solution was adopted as multi-scale corrosion expansion (MSCE) by increasing the corrosion scales. The MSCE algorithm was applied to a complicated image with many clusters of wear debris as shown in Fig. 13. A

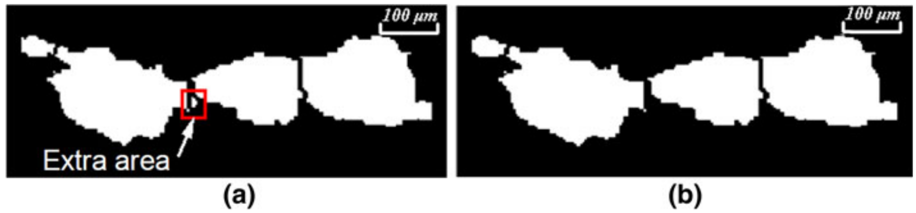

Fig. 12 The effect of post-processing by applying area-based filtering: **a** separation result, **b** area-based filtering result

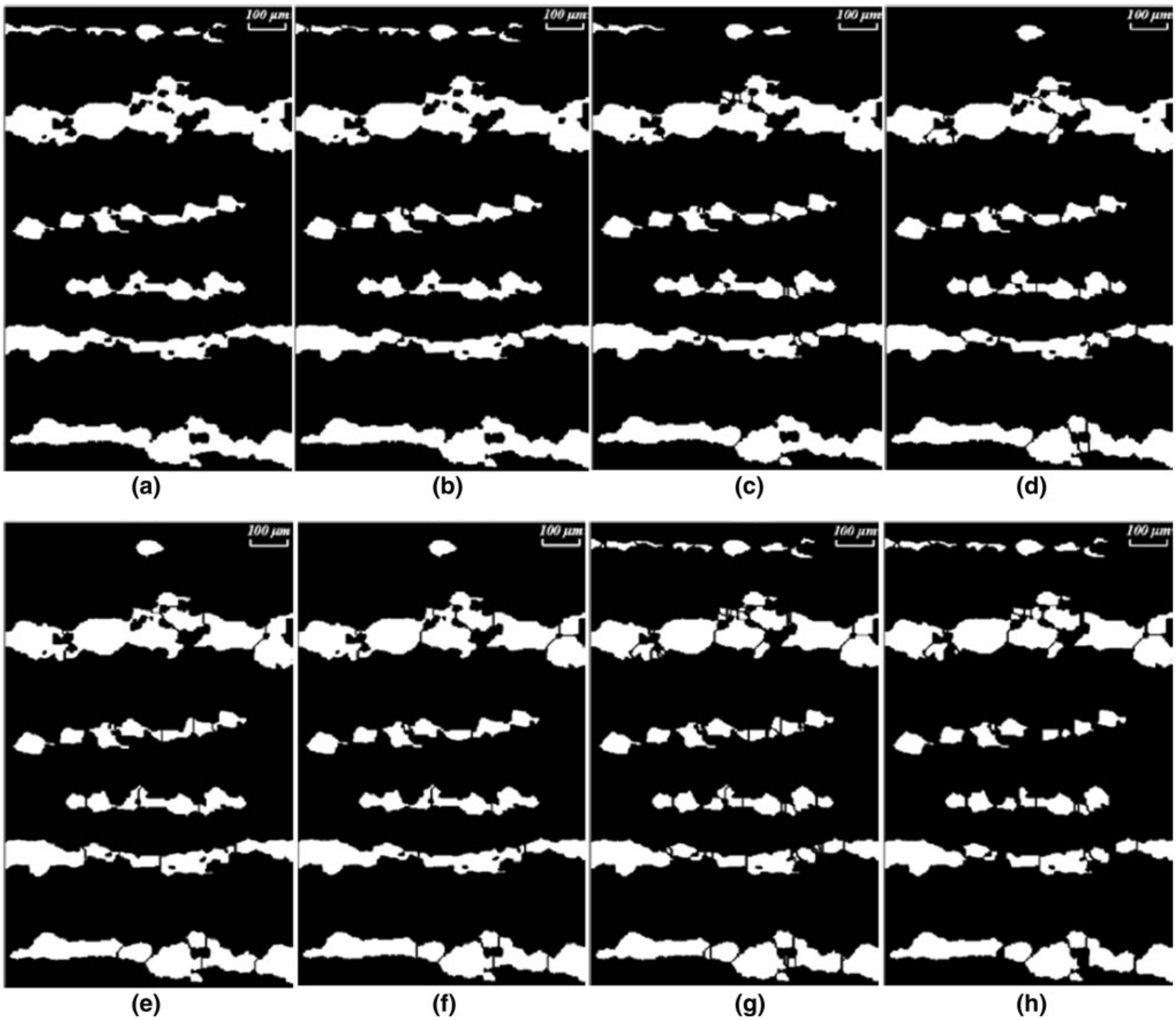

Fig. 13 Separation of wear debris by processing multi-corrosion expansion with different corrosion scales and post-processing: **a** initial image, **b** after corrosion with 1st scale, **c** after corrosion with 2nd scale, **d** after corrosion with 3rd scale, **e** after corrosion with 4th scale, **f** after corrosion with 5th scale, **g** integration of every scale, **h** after post-processing

typical image of wear debris with an extremely complicated pattern of chains was chosen as an illustration, see Fig. 13a, for automatic separation. Several corrosion-expansion cycles with total five corrosion scales were employed. In the former smaller scales, the dividing lines were short and only smaller wear debris was separated. With the separation continuing, the dividing lines became longer, and larger wear debris was separated. As seen in Fig. 13g, most wear debris was separated successfully. However, oversegmentation also appeared with many consistent small areas. Therefore, a post-processing procedure was carried out, and the result shows an improved effect, as shown in Fig. 13h.

Table 1 Statistical result of all individual wear debris features in Fig. 13

Statistics	A (μm^2)	P (μm)	AR	R	ECD (μm)
Maximum	17,415	735	8.3	3.6	149
Minimum	27	9	1.0	0.2	6
Median	2,187	177	1.7	1.1	53
Mean	3,879	214	2.0	1.3	59
SD	4,684	159	1.1	0.6	38
C.V (%)	121	75	57	44	66

A area: area measurement of wear debris; *P* perimeter: length of wear debris boundary; *AR* aspect ratio: it is a common measure of shape. $AR = L/W$; *R* roundness: it is a measure of how closely an object resembles a circle. $R = (4 \times A)/(\pi \times L^2)$; *ECD* equivalent circle diameter: it is a measure of the size of wear debris. $\mathrm{ECD} = (4 \times A/\pi)^{1/2}$; *SD* standard deviation: $\mathrm{SD} = \left(1/n \cdot \sum_{i=1}^{n} (x_i - \bar{x})^2\right)^{1/2}$ (x_i is the value of statistics; $\bar{x}$ is the mean of x_i; n is the number of characteristic value); *C.V* variation coefficients: $\mathrm{C.V} = (\mathrm{SD}/\mathrm{MEAN})\%$

Feature extraction is an important step both for on-line and off-line ferrograph analysis and was conducted after the wear debris chain was separated in this work. In fact, there are different features for characterizing wear debris but not all the features are necessary for classifying the particles [21]. To balance the accuracy and efficiency of the feature extraction for on-line analysis, only some distinctive features were considered in this study. The number of wear debris, as one of the primary features, can be extracted by counting the cores of the isolated wear debris. The morphological features of the separated wear debris include many indicators, especially the characteristics of larger wear debris in an image. Wear mechanism was related to these parameters in many studies [3–7]. Accordingly, some basic parameters for particle identification were selected as follows. Area and perimeter were used to characterize the size and shape feature of debris. Aspect ratio was employed to represent the cutting debris. Roundness and equivalent circle diameter were adopted as a typical indicator of spherical debris.

The features of the separated wear debris in Fig. 13h were extracted. Fifty-seven wear particles were obtained by applying the proposed method. All the above-mentioned parameters were applied to analyze the wear particles, which provide a base for particle classification. Following the individual particle characterizations, statistical analysis was conducted and the results are listed in Table 1. The distributions of the five parameters are shown in Fig. 14, respectively.

Nevertheless, some inherent problems with the morphological separation techniques remain unresolved. For instance, oversegmentation due to the irregular shape of the wear debris can be an issue. In addition, gray information, including the color and surface texture that are useful in determining the overlap and adhesion of wear debris, was not taken into consideration in this work. Therefore, fusion between the color and morphological information will be considered in future work to further improve the accuracy and efficiency of this particle separation technique.

5 Conclusion

Wear monitoring of complex and modern machinery demands on-line wear debris analysis. Although identifying and analyzing individual wear debris provide valuable information of wear mechanisms and wear modes for wear examination and cause analysis, particle separation and

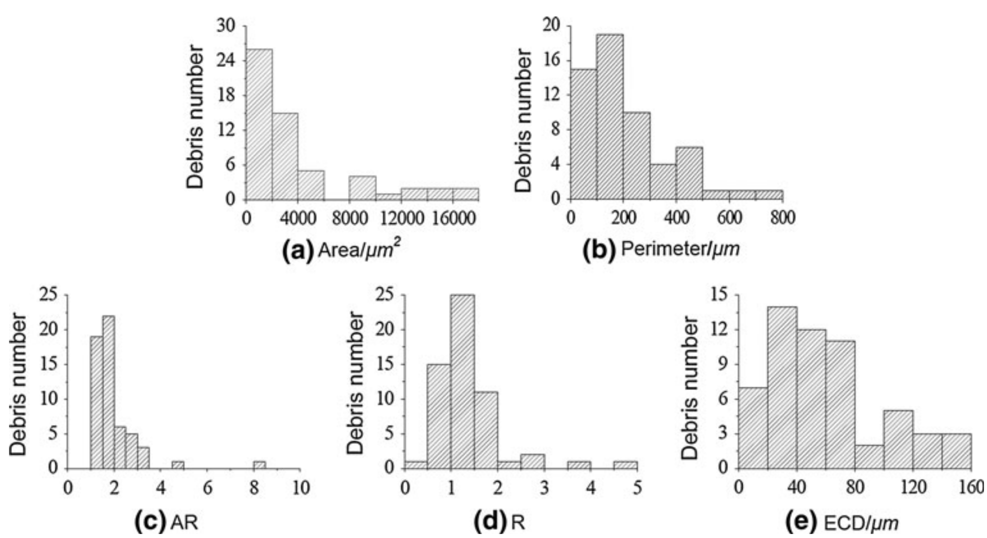

Fig. 14 Statistical results of feature extraction of all the debris in Fig. 13h: **a** area (*A*), **b** perimeter (*P*), **c** aspect ratio (*AR*), **d** roundness (*R*), **e** equivalent circle diameter (*ECD*)

classification remain the bottleneck for on-line visual wear debris analysis. Aiming at the separation of the imaged irregular and overlapping wear debris from chains in on-line ferrograph, the feasibilities of the morphological watershed methods were investigated. Improvements toward a high degree of accuracy and efficiency were made. Consequently, a synthesis method was proposed, and satisfactory outcomes of on-line separation of wear debris were achieved, with the primary conclusions outlined as follows:

1. The wide size range and the high irregularity of wear debris in an on-line image introduced major challenge to applying the reported methods to separate the wear debris. Distance-based methods have errors of oversegmentation that increases debris counting. Furthermore, ultimate corrosion-conditional expansion transformation results in an erroneous identification of dividing lines of separated wear debris and then leads to misidentification of the boundaries of wear debris.
2. An improved multi-scale corrosion-expansion method has been therefore proposed for on-line purposes. Compared with ultimate corrosion-conditional expansion, the proposed method has higher separation accuracy and efficiency by applying a flexible corrosion strategy. Instead of using a constant corrosion scale, but by adopting a varied scale, acceptable results have been obtained by primary examination with typical on-line ferrograph images.
3. The proposed method not only provides a feasible and improved technique to separate on-line particles for further analysis, but also allows for the statistical distributions of separated wear debris. The quantitative wear debris characterization overcomes the limitations of the qualitative analysis approach of traditional analytical ferrograph and fundamentally prompts the automation of on-line ferrography. In addition, the developed techniques can be used for off-line wear debris analysis and will contribute to the automation of off-line ferrography.

Acknowledgments The financial supports for the present research were provided by the National Science Foundation of China (Grant Nos. 51275381, 50905135), the China Scholarship Council (Grant No. 201206285002), and the Science and Technology Planning Project of Shaanxi Province, China (Grant No. 2012GY2-37). The author would also like to acknowledge all the members of the Tribology research group in the School of Mechanical & Manufacturing Engineering, the University of New South Wales for very helpful discussions. Special thanks to Pro. Weihua Li at the University of Wollongong for English polishing.

References

1. Jardine, A.K.S., Lin, D., Banjevic, D.: A review on machinery diagnostics and prognostics implementing condition-based maintenance. Mech. Syst. Signal Process. **20**(7), 1483–1510 (2006)
2. Levi, O., Eliaz, N.: Failure analysis and condition monitoring of an open-loop oil system using ferrography. Tribol. Lett. **36**(1), 17–29 (2009)
3. Raadnui, S.: Wear particle analysis—utilization of quantitative computer image analysis: a review. Tribol. Int. **38**(10), 871–878 (2005)
4. Hunt, T.M.: Handbook of Wear Debris Analysis and Particle Detection in Liquids. Springer, Berlin (1993)
5. Peng, Z., Kirk, T.B.: Computer image analysis of wear particles in three-dimensions for machine condition monitoring. Wear **223**(1), 157–166 (1998)
6. Stachowiak, G.P., Podsiadlo, P., Stachowiak, G.W.: Shape and texture features in the automated classification of adhesive and abrasive wear particles. Tribol. Lett. **24**(1), 15–26 (2006)
7. Peng, Z., Kirk, T.B.: Automatic wear-particle classification using neural networks. Tribol. Lett. **5**(4), 249–257 (1998)
8. Roylance, B.J.: Ferrography-then and now. Tribol. Int. **38**(10), 857–862 (2005)
9. Mujahid, A., Dickert, F.L.: Monitoring automotive oil degradation: analytical tools and onboard sensing technologies. Anal. Bioanal. Chem. **404**(4), 1197–1209 (2012)
10. Wu, T.H., Wang, J.Q., Peng, Y.P., Zhang, Y.L.: Description of wear debris from online ferrograph images by their statistical color. Tribol. Trans. **55**(5), 606–614 (2012)
11. Wu, T.H., Mao, J.H., Wang, J.T., Wu, J.Y., Xie, Y.B.: A new on-line visual ferrograph. Tribol. Trans. **52**(5), 623–631 (2009)
12. Jin, L., Wang, J.Q., Wang, C.: The technical research of ferrography division of morphology. Softw. Eng. Knowl. Eng.: Theory Pract. **114**, 1027–1037 (2012)
13. Bleau, A., Leon, L.J.: Watershed-based segmentation and region merging. Comput. Vis. Image Underst. **77**(3), 317–370 (2000)
14. Vincent, L.: Morphological grayscale reconstruction in image analysis: applications and efficient algorithms. IEEE Trans. Image Process. **2**(2), 176–201 (1993)
15. Visen, N.S., Shashidhar, N.S., Paliwal, J., Jayas, D.S.: AE—automation and emerging technologies: identification and segmentation of occluding groups of grain kernels in a grain sample image. J. Agric. Eng. Res. **79**(2), 159–166 (2001)
16. Feng, L.J., Yu, Y.J., Min, T.Z., Yu, K.Y., Dong, W.: Design of a separating algorithm for overlapping cell images. J. Comput. Res. Dev. **2**, 228–232 (2000)
17. Anoraganingrum, D., Kröner, S., Gottfried, B.: Cell Segmentation with Adaptive Region Growing, pp. 27–29. ICIAP Venedig, Italy (1999)
18. Van den Berg, E.H., Meesters, A.G.C.A., Kenter, J.A.M., Schlager, W.: Automated separation of touching grains in digital images of thin sections. Comput. Geosci. **28**(2), 179–190 (2002)
19. An, N., Cong, P., Zhu, Z.: Wheat quality recognition based on watershed algorithm and kernel partial least squares. Nat. Comput. **2**, 265–269 (2009)
20. Serra, J.: Morphological filtering: an overview. Signal Process. **38**(1), 3–11 (1994)
21. Wang, J., Wang, X.: A wear particle identification method by combining principal component analysis and grey relational analysis. Wear **304**, 96–102 (2013)